Fibers and Polymers 2021, Vol.22, No.5, 1441-1448
DOI 10.1007/s12221-021-0521-0

ISSN 1229-9197 (print version)
ISSN 1875-0052 (electronic version)

Investigation of Tensile Properties of Glass Fiber/Epoxy Nanocomposites Laminates Enhanced with Graphene Nanoparticles

Mehmet Çağrı Tüzemen*, Farnoud Khakzad, and Elmas Salamci

Department of Mechanical Engineering, Gazi University, Ankara 06570, Turkey
(Received May 7, 2020; Revised July 28, 2020; Accepted August 17, 2020)

Abstract: In this study, mechanical properties of graphene nanoparticles (GNP) added glass fiber/epoxy nanocomposite specimens and the effect of GNP were investigated by applying the tensile test. Specimens were produced by vacuum assisted resin transfer molding (VARTM) method on the CNC device in standard sizes. The results obtained from the tensile test of the specimens prepared with the addition of GNP at the rates of 0.15 %; 0.25 %; 0.35 %; 0.45 % and 0.75 % were compared with the sample without GNP. According to the test results, the tensile strength increases with the increase in the rate of GNP. The highest tensile strength was found when the GNP rate was 0.45 %. At this rate, the tensile strength increases by 31.29 % compared to the specimens without additives. However, increasing the rate of GNP more than 0.45 % affects the mechanical properties negatively and causes a decrease in tensile strength. Finally, finite element analysis (FEA) was made by designing the produced specimens. FEA results were compared and found to be compatible with the experimental results.

Keywords: Graphene, Glass fibers, Mechanical properties, Nanoparticles, Vacuum assisted resin transfer molding

Introduction

The use of composites is ever more common due to their superior mechanical properties and because of the diversity of the offered composites. Composite materials can exhibit superior mechanical, thermal, electrical, and magnetic properties without compromising their lightweight. Material science is, however, advancing and pushing boundaries day by day. A composite material consisting solely of fiber and matrices may not always exhibit the desired mechanical properties. For the time being, nanoparticles are being used to improve the properties of composite materials. Nanoparticles are various particles with at least one dimension in the nano order. One can consider carbon nanotubes (CNT), nanoclay (NC), graphene nanoparticle or nanographene (GNP), and graphene oxide (GO), together with a wide variety of nanoparticles in fiber/epoxy composites, as nanoparticles that are frequently encountered in the literature [1-10].

In recent years, there have been studies on the changes in the mechanical properties of composites with the addition of graphene and its derivatives to the matrix [11-23]. Li *et al*. studied the effect of three different rates (0.1 %, 0.2 %, and 0.5 % by weight) of functionalized graphene oxide (GO) addition on the mechanical properties. They stated that the tensile strength and modulus of elasticity increased as the additive ratio increased [23]. Zakaria *et al*. examined the effect of three different rates (0.5 %, 1 %, and 3 % by weight) of GNP and multiwall carbon nanotube (MWCNT) addition on mechanical, thermal, and dielectric properties. The highest tensile strength and tensile modulus was obtained with 1 % wt. GNP addition among the GNP added specimens. A GNP addition of more than 1 % wt. leads to a decrease in tensile strength. They attributed this decrease, as the addition rate increased, to the agglomeration caused by Van der Waals forces. These agglomerations prevent stress distribution and lead to stress concentration. As a result, the matrix weakened [13]. Li and Xiong examined the effect of 0.25 %, 0.5 %, and 1 % wt. addition on microstructure and tensile mechanical properties. They reported that 0.25 wt% of the GNPs added to the aluminum matrix showed the highest tensile strength [14]. Liang investigated the effect of tension rates and filler size on mechanical properties. Five different samples were prepared for each parameter: 0.1 % 0.2 %, 0.3 %, 0.4 %, and 0.5 % by weight. As a result of the tensile test with tension rates of 100 mm/min, for all three filler sizes, the maximum tensile stress and the slope of the tensile stress-strain curves around the origin of coordinate system increase with increasing GNPs weight fraction [15].

Glass fiber/epoxy composites are used in many areas as they have high specific strength, electrical insulation, corrosion resistance, thermal properties, and are cheaper than other fibers such as carbon and aramid [24,25]. By adding nanoparticles to the glass fiber/epoxy composites, their mechanical and electrical properties are improved and thus their usage areas are further increased [26,27]. Haque *et al*. [28] found a 44 % shear strength increase between layers by adding 1 % nanosilicate to the glass/epoxy composite material. The increase was explained by the increase of the contact area between the surfaces and the improvement of the bonding properties. The effect of nanosilica on epoxy glass composite material (unidirectional) has been studied by Uddin and Sun [29]. The addition of 15 % nanosilica led to a significant increase in compressive strength and elastic modulus. Karippal *et al*. [30] added NC to the glass/epoxy composite material. The addition of up to 5 % nanoclay led to an increase in tensile strength, elasticity modulus, bending modulus, durability, and interlayer shear strength, but when added more than 5 % it causes the mechanical properties to

*Corresponding author: cagrituzemen@gazi.edu.tr

decrease. Zulfli *et al*. [31] examined the mechanical properties of glass/epoxy composites reinforced with calcium carbonate nanoparticles. The results of the impact and bending tests show that the elastic modulus and thermal decomposition temperature of the nanocomposite material is quite high when compared with the additive-free sample. In the glass-epoxy hybrid nanocomposites combined with CNT, elasticity modulus and durability increase according to the results obtained by bending and tensile tests. Hoseini and Pol [32] produced glass/epoxy composites containing NC particles by vacuum-assisted resin transfer molding (VARTM). It was determined that the most increase in tensile and bending properties was in the addition of 3 % and 7 % of NC. Salehi and Salehi [33] produced glass-epoxy hybrid nanocomposite reinforced with titanium oxide nanoparticles and investigated their mechanical properties. When the microstructures of hybrid nano composites are examined, it is seen that with the addition of nanoparticles, the contact surface of the fiber and matrix increases significantly, thereby increasing the adhesiveness between the fiber and the matrix.

Over the past few years, many studies have been published on the mechanical properties of NC and CNT additives. Although there are fewer studies related to GNP, they have begun to work intensively due to the superior mechanical properties of composites. The publications related to the tensile strength of the GNP added glass fiber/ epoxy nanocomposite and its finite element analysis (FEA) validation, nonetheless, are limited. To contribute to the literature, some investigations are now being done on the influences of certain GNP contributions on fiber/epoxy composites. In this study, GNP added glass fiber/epoxy nanocomposites were produced at different GNP ratios. Nanocomposite plates were produced by vacuum-assisted resin transfer molding (VARTM) method and specimens were prepared by cutting plates with computer numerical control (CNC) machines. The tensile strength of the nanocomposite was examined by the tensile test. The results obtained from the tests were consequently compared with the nanographene-free reference sample. In addition, FEA is performed, and verification of experimental data was provided.

Experimental

In the present work, glass fiber was used as a reinforcing element, epoxy was used as a matrix and nanographene particles as a reinforcer. Glass fiber fabric, F-1564 resin, and F-3468 hardener used in this study was obtained from Fibermak Kompozit. Glass fiber and epoxy have tensile strength of 2306 MPa and 70-80 MPa, elongation of 2.97 % and 5-6.5 %, and modulus of elasticity of 81.5 GPa and 3-3.3 GPa, respectively. The diameter of the glass fiber is 17 μm and the glass content is 62.1 %. GNP (GRAFEN®-iGP2) particles used in the present study were obtained from Graphene Factur Engineering. The GNP has an average particle diameter of 5-10 μm, and an average thickness of 5-10 nm.

Graphene-Epoxy Mixing

For homogenous mixing of the nanographene in the epoxy, the nanographene was first added to the epoxy in five different fractions which are 0.15 %, 0.25 %, 0.35 %, 0.45 %, and 0.75 % by weight and the mixture was stirred for about 2 h at 45 °C by a magnetic stirrer, and at the second stage for about 1 h at 45 °C in an ultrasonic mixing apparatus. This method is performed to eliminate nanographene aggregation. Mechanical, ultrasonic and magnetic stirrers are used in the literature for the homogeneous distribution of nanoparticles [34-38]. One of the recent studies has shown that ultrasonic mixing is the most effective way [37]. Magnetic and ultrasonic mixing approaches were used together in another experiment to achieve homogeneous mixing [38]. Hence, the mixing methods used in this study can be said to be an appropriate approach for the homogeneous distribution of nanoparticles. Then the hardener is added to the resin and mixed by hand for about 10 min. The resin-hardener ratio is 100:34.

Composite Production

The VARTM method was applied in the production of the specimens used in this study (Figure 1). This method is commonly used in the literature [39-44]. Firstly, the counter surface was completely cleaned. The release film was laid first, then the eight layers of glass fiber fabrics, which are twill woven fabrics having the same orientation for 0 ° and 90 ° directions, were placed one by one on top of it. Peel ply, flow mesh, and vacuum bag were laid on top of them, respectively. Spiral and vacuum hoses were connected. The resin entering the inlet was absorbed into the fibers by vacuum. After absorption and penetration of the nanographene-resin mixture into the glass fiber fabric, curing was done for 1 h at 100±5 °C. The system reached 100 °C in about half an hour and after 1 h curing at 100 °C, it went down to room temperature in about 1 h. In the experimental program, no additive specimen (GNP0) and specimens prepared with 0.15 % (GNP15); 0.25 % (GNP25); 0.35 % (GNP35); 0.45 % (GNP45), and 0.75 % (GNP75) wt% nanographene addition were used. Eighteen test samples were produced in the form of three repeats.

Experimental Methods

Ashing test was applied to determine the volume fractions of fiber (V_f), matrix (V_m), and void (V_v) of the nanocomposite. The test was conducted according to ASTM D2734 and ASTM D2584 standards [45,46]. The specimens were cut in the size of 25×25 mm. For each composition, three replicates were tested. The weight of specimens was measured, and volumes were calculated by using sample size. Specimens

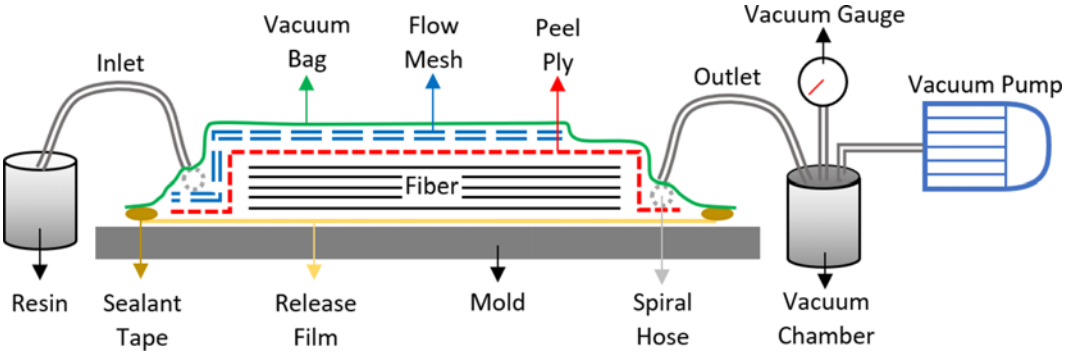

Figure 1. Schematic diagram of the VARTM method.

were then burned to remove epoxy at 560 °C. The remaining glass fibers of the specimens were weighed again and V_f, V_m, and V_v were calculated (Table 1).

The tensile test is performed in accordance with ASTM D3039/D3039M standards [47]. The size, width, and thickness of the test specimens are 250 mm, 25 mm, and 2 mm respectively, as specified in the standards. The tests were conducted on Shimadzu test equipment located in TOBB University Faculty of Engineering Department of Mechanical Engineering Laboratories (Figure 2). For each composition, three replicates were tested. The feed rate was determined as 2 mm/min.

Table 1. Volume fraction of the components of nanocomposite plates

Specimen	V_f	V_m	V_v
GNP0	68.03±3.4	30.62±1.5	1.15±0.06
GNP15	66.95±2.7	31.23±1.3	1.82±0.07
GNP25	66.47±4.7	31.49±2.2	2.04±0.14
GNP35	66.24±4.3	31.65±2.1	2.11±0.13
GNP45	65.85±3.6	31.67±1.7	2.48±0.11
GNP75	63.61±5.7	32.87±2.9	3.51±0.28

Figure 2. Nanocomposite specimen broken during the tensile test.

Numerical Analysis

For FEA, a model of the dimensions of the tensile sample was made first. The needed material was selected as epoxy glass fiber from the program library. Eight layers were identified, just as the specimens. However, the material properties in the library only apply to the nanoparticle-free model. Material properties such as modulus of elasticity and tensile strength for nanoparticle added models were edited according to the results obtained from the experiments. Also, preliminary analyses were carried out to ensure independence from mesh size. As a result of preliminary analysis, the model was meshed and divided into elements. The analysis is basically done by calculating the stresses caused by the loads on these elements one by one in the background. As a result of tensile tests, data were obtained only for the axis in the tensile direction. Based on the features reported by Kachlakev for the other axes, features related to these axes were entered the program [48]. The fix supports and the force inputs required to simulate the tensile test were applied to the model. Force inputs were entered the program as a tabulated force data obtained from the tensile test.

Results and Discussion

Volume fractions of the nanocomposite samples are shown in Table 1. As the GNP increases, it is seen that V_f decrease and V_m and V_v increase. The reason for this is that GNP contribution increases the density of epoxy. It has been reported that 10 % by weight nanoparticle additive increases the content of epoxy by 3 % [49]. The increase in the density

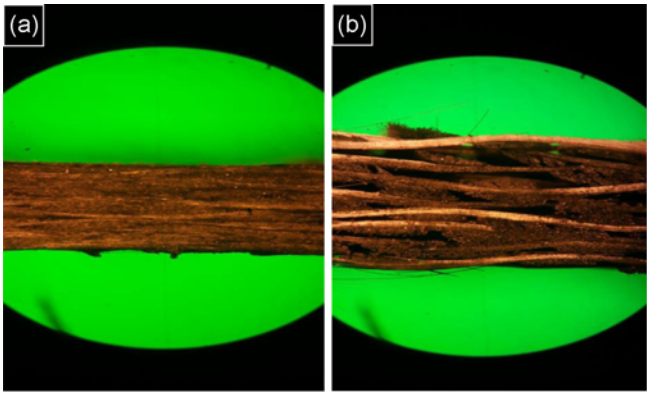

Figure 3. Side view of the graphene-added sample (a) before ashing test and (b) after ashing test.

of epoxy makes it difficult for the excess epoxy remaining in the system to exit from the system under vacuum. Therefore, the matrix volume ratio increases and the fiber volume ratio decreases. Although the two-stage mixing process has been made, the increase in GNP addition increases the likelihood of GNP clusters. These clusters can be attached to the fibers during the vacuum process. As a result, epoxy flow in this area is interrupted and small air gaps can form. For this reason, it can be said that as the GNP ratio increases, the V_v increases [39]. Figure 3 shows the graphene-added specimen before and after the ashing test.

The results of the tensile tests are shown in Table 2. According to the results, an increase in tensile strength is observed with the increase of GNP. However, due to the addition of more nanoparticles after 0.45 % GNP addition, the amount of increase in tensile strength decreased. The reasons for this can be said to be the agglomeration and an increase in V_v. The increase in V_v increases as GNP contribution increases. However, these increases are limited up to 0.45 % contribution. A faster upward trend is observed after this rate. As the GNP contribution increases, it is seen that the decrease in fiber volume ratio increases with the increase in porosity (Table 1). Therefore, it can be said that the GNP contribution increases the tensile strength by positive effect at low rates, while the effect at high rates turns negative. The lowest tensile strength was obtained in the GNP0 with 361.21 MPa. The highest tensile strength was obtained in the GNP45 with 474.24 MPa. This value shows that 0.45 % GNP addition increases the tensile strength by 31 % compared to the specimen without GNP addition. The increase in tensile strength of GNP15, GNP25, and GNP35 was 12 %, 19 %, and 24 %, respectively. The increase in GNP75 remained at 21 %. This value is between GNP25 and GNP35. These results show that the addition of GNP after a certain ratio does not increase the tensile strength of the composite further. It may even cause it to decrease. This optimum value was found to be 0.45 % GNP addition in this study.

A similar effect can be mentioned for the strain and the toughness values of the nanocomposite specimens. Toughness values were calculated from the area under the stress-strain curves. When the toughness values were examined, a continuous increase was observed up to 45 % GNP added specimen. However, more GNP additions led to a decrease in this increase, although it still increased compared to the GNP-free specimen GNP0. Compared to the GNP0, the increase in toughness value is 22 % for GNP15, 37 % for GNP 25, 55 % for GNP45, 76 % for GNP45 and 36 % for GNP 75. The modulus of elasticity of the specimens was calculated based on the linear part of the first stage of the stress-strain curve. The highest modulus of elasticity comes out in the GNP45 and the second one is the GNP75. The increase in modulus of elasticity of GNP15, GNP25, GNP35, GNP45, and GNP75 compared to GNP0 was 26 %, 36 %, 33 %, 44 %, and 37 %, respectively.

The stress-strain graph of the tensile test that consists of

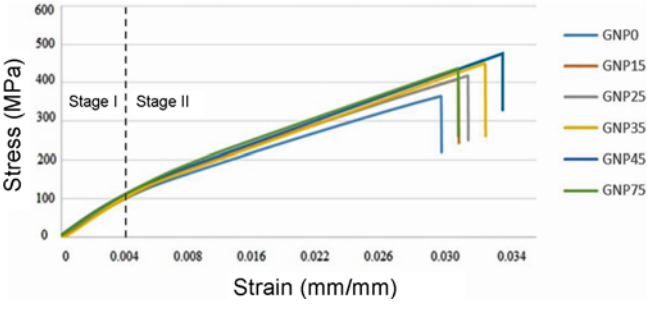

Figure 4. Stress-strain curves of nanocomposites.

Table 2. Tensile test results

Specimen	Stress (MPa)	Strain (mm/mm)	Modulus of elasticity (GPa)	Toughness (MJ/m^3)
GNP0	361.21±18.06	0.02624±0.0013	19.54±0.98	4.94±0.25
GNP15	404.06±28.28	0.02862±0.0020	24.61±1.72	6.05±0.42
GNP25	431.13±17.25	0.02941±0.0012	26.56±1.06	6.78±0.27
GNP35	447.92±24.64	0.02938±0.0016	26.08±1.43	7.66±0.42
GNP45	474.24±30.83	0.03116±0.0020	28.13±1.83	8.71±0.57
GNP75	437.39±39.37	0.02836±0.0026	26.83±2.41	6.72±0.60

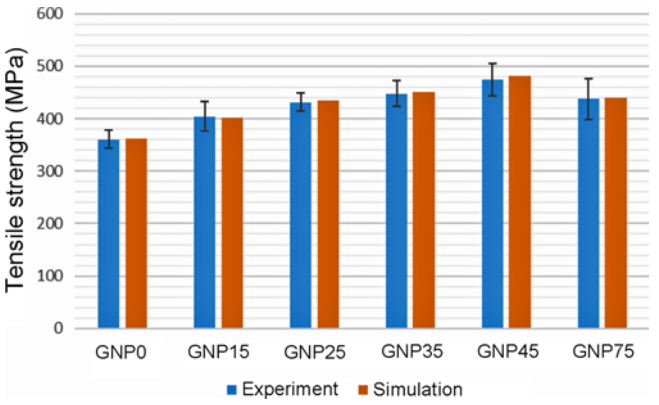

Figure 5. Experimental and analysis results obtained from the tensile test.

two stages is shown in Figure 4. In the first stage, both the epoxy matrix and the glass fibers exhibit elastic behavior. In the second stage, the epoxy resin yields and undergoes plastic deformation. The glass fibers are still in the elastic region. The curves in this graph continue linearly until the second stage. The slope decreases in the second phase and continues almost linearly [50].

A graphical comparison of the tensile strength results of the experimental and the FEA is given in Figure 5. Just like the experimental result, the biggest increase in tensile strength was observed in the GNP45 for the analysis. The rate of increase in tensile strength compared to GNP0 has continuously increased up to GNP45. However, the rate of increase in GNP75 decreased. As can be seen in Figure 5, the results of the analysis were found to be quite close to the average value of the experimental results. The greatest difference between the experiment and analysis remained at 2 %. These differences remain within the error bars obtained as a result of the experimental study. This shows that the approach in the analysis is quite successful.

As shown in Figure 6, fracture of the samples in the axial load occurs due to fiber rupture. Also, fiber fragmentation occurs in the fracture area. In this experiment, delamination on the fracture surface is not observed. The reason is that all layers are subjected to axial tensile loads during the test. The

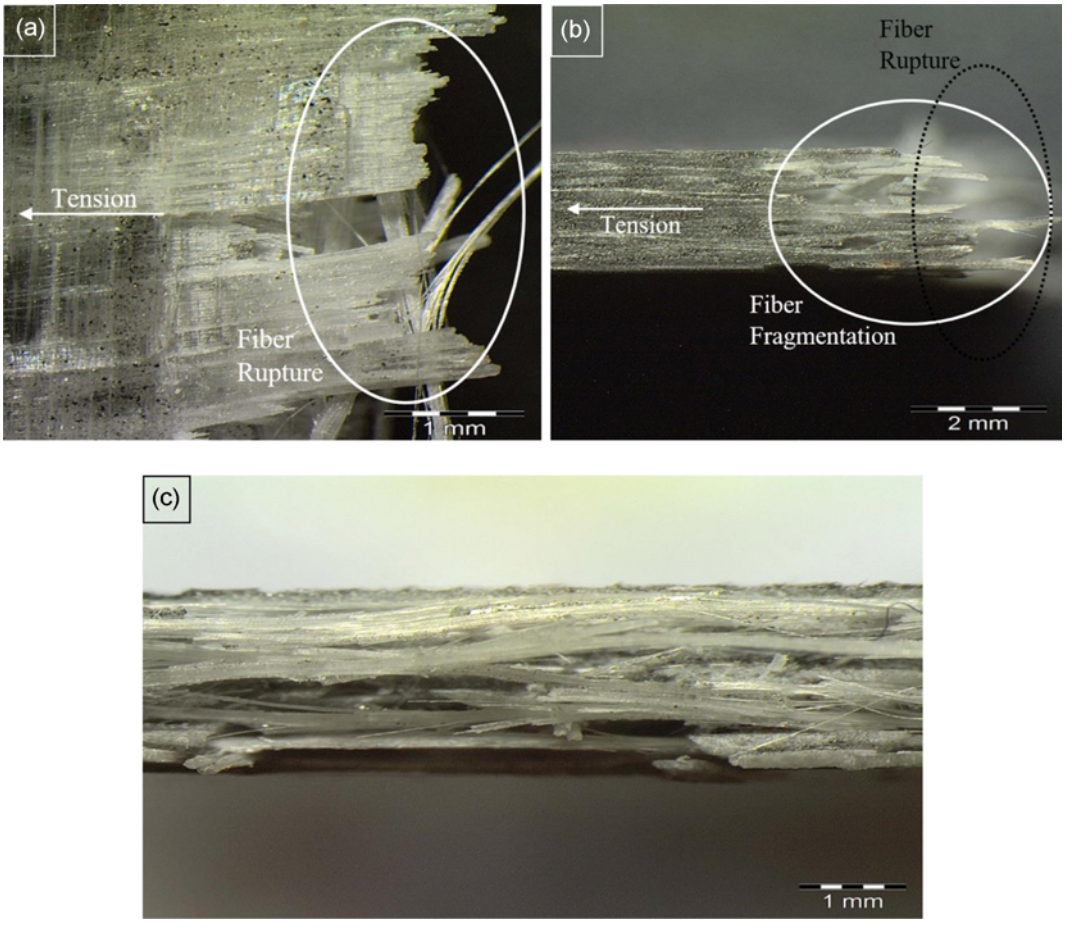

Figure 6. (a) Top, (b) side, and (c) front view optical microscope image taken from the fracture surface of the GNP25 sample after the tensile test.

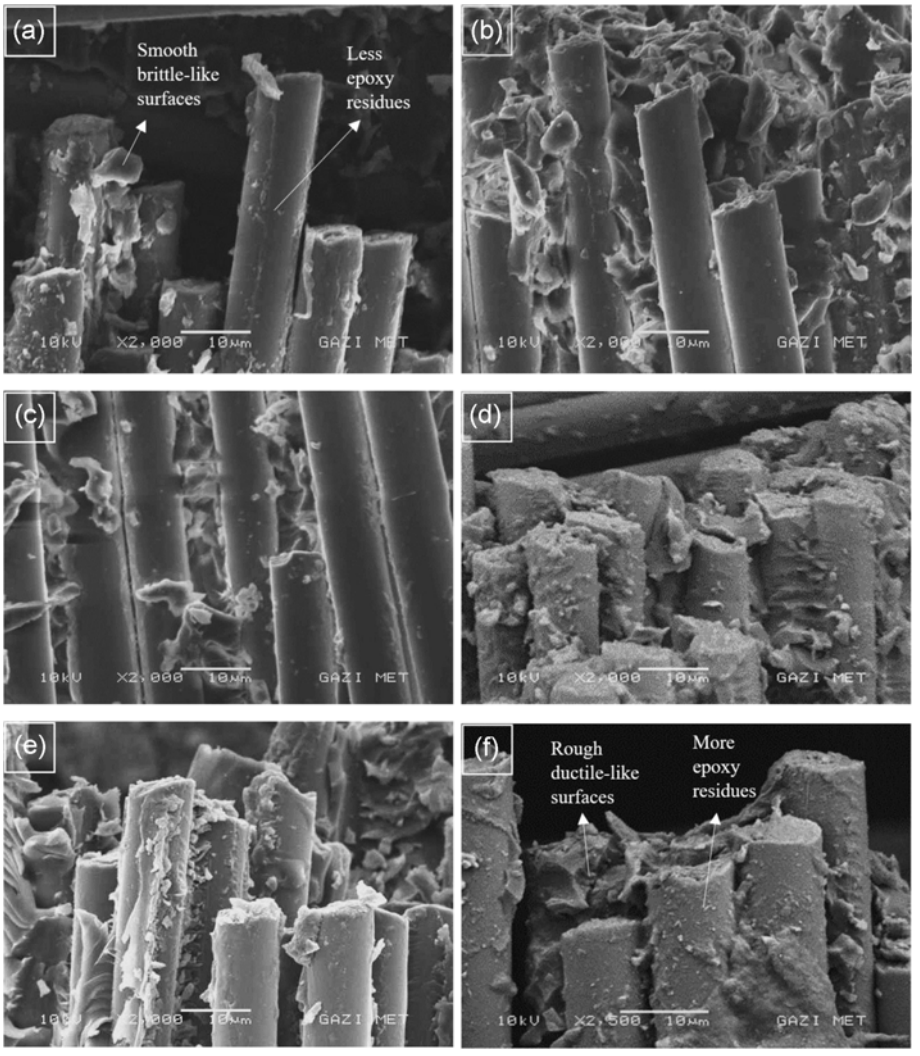

Figure 7. SEM images taken perpendicular to the fracture surface of the tensile test specimens; (a) GNP0, (b) GNP15, (c) GNP25, (d) GNP35, (e) GNP45, and (f) GNP75.

tension between the layers is low, so it has been found that the fiber rupture has a major role in fracture. After the tensile test, the test specimens were examined by SEM. All the SEM images were taken from the fracture surface and areas. SEM image was taken from the perpendicular (Figure 7) and axial (Figure 8) direction to the damaged areas on the fractured surface of the tensile test specimens.

When SEM images are examined, epoxy surfaces show smooth and brittle-like behavior in the specimens with no nano additives and relatively less GNP additives. As the GNP ratio increases, these surfaces start to show rough and ductile-like behavior. It can be said that the transition from brittle-like behavior to ductile-like behavior shows how the GNP additive improves its mechanical properties. As the GNP additive increases, more epoxy residues sticking on the fibers are observed. This shows that stronger bonds are formed between fiber and epoxy resin. Therefore, considering that the main damage mechanism under tensile load is fiber breakage, the strengthening of the bond between the fibers and the epoxy resin supports the increase in strength obtained as a result of the experiment. In fact, while the GNP additive directly affects only the epoxy resin, it can be said that it indirectly affects the fibers thanks to the strengthening of the bonds between the epoxy and fiber. Thus, even if the main damage mechanism is fiber breakage, GNP additives increase the nanocomposite's strength. However, as explained earlier, the improvement in mechanical properties is valid as long as there is a GNP addition up to a certain rate. The likelihood of voids in the matrix can increase due to agglomeration. These cavities act like cracks, which can cause the material to be damaged at lower loads. The GNP75 sample was able to withstand lower forces than samples with less GNP containing like GNP35 and GNP45. It is thought that agglomeration may be caused.

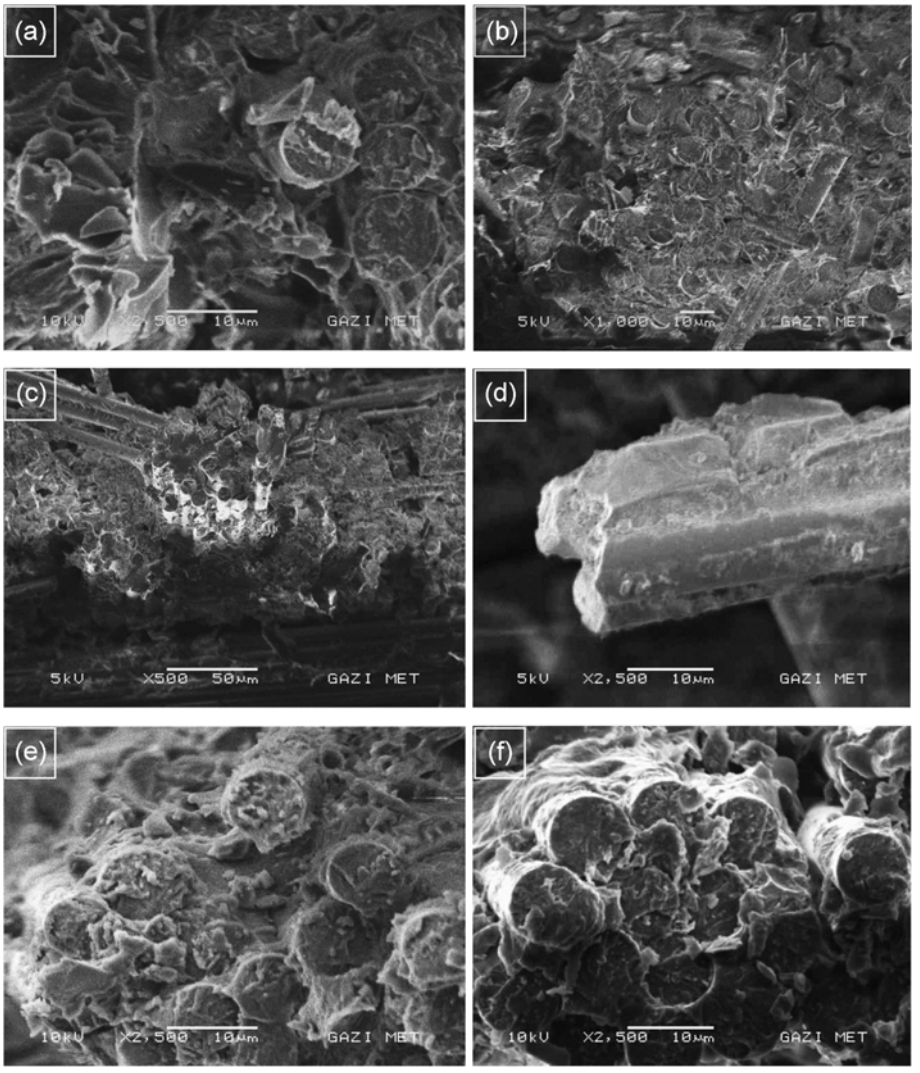

Figure 8. SEM images of tensile test specimens in the axial direction from fracture surface; (a) GNP0, (b) GNP15, (c) GNP25, (d) GNP35, (e) GNP45, and (f) GNP75.

Conclusion

In this study, the behaviors of nanocomposite specimens with different GNP ratios were investigated under axial load. As a production method, VARTM, which is frequently used in the literature and enables high fiber volume ratios, was used.

According to the ashing test results, as the GNP ratio increases, V_f decreases, V_m and V_v increase. The increase in the V_v shows that with the increase in the GNP ratio, the voids in the nanocomposite plates increase. Nevertheless, the VARTM method allows the production of specimens with a high V_f. As the nanographene ratio increased to 0.45 %, the tensile strength increased almost linearly. However, the addition of 0.75 % graphene stopped this upward trend and even decreased it. The highest tensile strength was determined at the GNP45 test specimen. In this specimen, tensile strength, deformation, modulus of elasticity and toughness increased by 31.29 %, 18.75 %, 43.96 %, and 76.3 %, respectively. The price of the nanographene added plate produced for this specimen was $ 24.74 and increased approximately $ 4.74 compared to the nanographene-free reference plate. Nanographene additive increases the price of the specimen by approximately 24 %. Therefore, it increases the mechanical properties more than the price while increasing its weight by only less than 0.45 %. Finally, FEA approach gave results close to those obtained in the tensile test.

References

1. E. H. Lee, M. H. Jee, C. S. Kang, and D. H. Baik, *Fiber.*

Polym., **20**, 832 (2019).
2. V. Datsyuk, S. Trotsenko, G. Trakakis, A. Boden, K. Vyzas-Asimakopoulos, J. Parthenios, C. Galiotis, S. Reich, and K. Papagelis, *Polym. Test.*, **82**, 106317 (2020).
3. J. W. Lee, J. U. Lee, J. W. Jo, S. Bae, K. T. Kim, and W. H. Jo, *Carbon*, **105**, 191 (2016).
4. J. Bhinder and P. K. Agnihotri, *J. Appl. Polym. Sci.*, **137**, 48736 (2019).
5. T. A. Zidan, *Polym. Compos.*, **41**, 564 (2020).
6. R. Karakuzu, B. Algan, and M. E. Deniz, *Materialpruefung/ Materials Testing*, **61**, 231 (2019).
7. A. Nazari, *Fiber. Polym.*, **20**, 2618 (2019).
8. W. Liang, F. Wang, T. E. Tay, B. Yang, and Z. Wang, *Polym. Eng. Sci.*, **60**, 233 (2020).
9. M. M. Alrashed, M. D. Soucek, and S. C. Jana, *Progr. Org. Coat.*, **134**, 197 (2019).
10. F. Alimohammadi, M. Parvinzadeh Gashti, and A. Mozaffari, *Fiber. Polym.*, **19**, 1940 (2018).
11. L. P. Lim, J. C. Juan, N. M. Huang, L. K. Goh, F. P. Leng, and Y. Y. Loh, *Mater. Sci. Eng. B: Solid-State Mater. Adv. Technol.*, **246**, 112 (2019).
12. S. Chhetri, N. C. Adak, P. Samanta, N. C. Murmu, and T. Kuila, *Polym. Test.*, **63**, 1 (2017).
13. M. R. Zakaria, M. H. Abdul Kudus, H. Md. Akil, and M. Z. Mohd Thirmizir, *Compos. Part B: Eng.*, **119**, 57 (2017).
14. G. Li and B. Xiong, *J. Alloys Compd.*, **697**, 31 (2017).
15. J. Z. Liang, *Compos. Part B: Eng.*, **167**, 241 (2019).
16. Y. J. Wan, L. C. Tang, L. X. Gong, D. Yan, Y. B. Li, L. Bin Wu, J. X. Jiang, and G. Q. Lai, *Carbon*, **69**, 467 (2014).
17. M. Yan, W. Jiao, G. Ding, Z. Chu, Y. Huang, and R. Wang, *Appl. Surface Sci.*, **497**, 143802 (2019).
18. J. Cha, J. Kim, S. Ryu, and S. H. Hong, *Compos. Part B: Eng.*, **162**, 283 (2019).
19. J. P. Long, S. X. Li, B. Liang, and Z. G. Wang, *Plast. Rubber Compos.*, **48**, 127 (2019).
20. S. I. Abdullah and M. N. M. Ansari, *HBRC J.*, **11**, 151 (2015).
21. N. C. Adak, S. Chhetri, S. Sabarad, H. Roy, N. C. Murmu, P. Samanta, and T. Kuila, *Compos. Sci. Technol.*, **177**, 57 (2019).
22. N. T. Kamar, M. M. Hossain, A. Khomenko, M. Haq, L. T. Drzal, and A. Loos, *Compos. Part A: Appl. Sci. Manuf.*, **70**, 82 (2015).
23. Z. Li, R. Wang, R. J. Young, L. Deng, F. Yang, L. Hao, W. Jiao, and W. Liu, *Polymer*, **54**, 6437 (2013).
24. D. Gay, *Compos. Mater.: Des. Appl.*, **3**, 203 (2014).
25. J. M. Stickel and M. Nagarajan, *Int. J. Appl. Glass Sci.*, **3**, 122 (2012).
26. M. H. G. Wichmann, J. Sumfleth, F. H. Gojny, M. Quaresimin, B. Fiedler, and K. Schulte, *Eng. Fract. Mech.*, **73**, 2346 (2006).
27. T. Hanemann and D. V. Szabó, *Materials*, **3**, 3468 (2010).
28. A. Haque, M. Shamsuzzoha, F. Hussain, and D. Dean, *J. Compos. Mater.*, **37**, 1821 (2003).
29. M. F. Uddin and C. T. Sun, *Compos. Sci. Technol.*, **68**, 1637 (2008).
30. J. J. Karippal, H. N. N. Murthy, K. S. Rai, M. Sreejith, and M. Krishna, *J. Compos. Mater.*, **45**, 1893 (2011).
31. N. H. M. Zulfli, A. A. Bakar, and W. S. Chow, *High Perform. Polym.*, **26**, 223 (2014).
32. S. A. V. Hoseini and M. H. Pol, *Modares Mechanical Engineering*, **14**, 103 (2014).
33. H. R. Salehi and M. Salehi, *Iran. J. Polym. Sci. Technol.*, **28**, 263 (2015).
34. F. Khakzad, M. Ç. Tüzemen, E. Salamci, and Ö. Anıl, *Polym. Eng. Sci.*, **59**, 2082 (2019).
35. A. Kumar, S. Li, S. Roy, J. A. King, and G. M. Odegard, *Compos. Sci. Technol.*, **114**, 87 (2015).
36. K. K. Singh, S. K. Chaudhary, and R. Venugopal, *Polym. Eng. Sci.*, **59**, E248 (2019).
37. B. Zhang and T. Chen, *Materials*, **12**, 1757 (2019).
38. Ö. B. Mergen, E. Arda, S. Kara, and Ö. Pekcan, *Polym. Compos.*, **40**, 1862 (2019).
39. M. Ç. Tüzemen, E. Salamci, and A. Avci, *Gazi Üni. Fen Bil. Der. Part C: Tas. Teknol.*, **5**, 11 (2017).
40. A. Thiagarajan, K. Jagadish Chandra Bose, K. Velmurugan, and V. S. K. Venkatachalapathy, *Adv. Manuf. Technol.*, https://doi.org/10.1007/978-981-13-6374-0_41 (2019).
41. J. I. Kim, Y. T. Hwang, K. H. Choi, H. J. Kim, and H. S. Kim, *Compos. Struct.*, **211**, 236 (2019).
42. M. A. Yalcinkaya, E. M. Sozer, and M. C. Altan, *Polym. Compos.*, **40**, 2482 (2019).
43. Ö. F. Erkendirci and A. Avcı, *Plastics, Rubber and Composites*, **49**, 25 (2020).
44. M. Ç. Tüzemen, E. Salamcı, and A. Avcı, *Compos. Part B: Eng.*, **128**, 146 (2017).
45. ASTM D2734-94, "Standard Test Methods for Void Content of Reinforced Plastics", ASTM International, West Conshohocken, PA, 1994.
46. ASTM D2584-11, "Standard Test Method for Ignition Loss of Cured Reinforced Resins", ASTM International, West Conshohocken, PA, 2011.
47. ASTM D3039/D3039M-17, "Standard Test Method for Tensile Properties of Polymer Matrix Composite Materials", ASTM International, West Conshohocken, PA, 2017.
48. D. I. Kachlakev, FHWA-OR-RD-98-08, Oregon Department of Transportation, Salem, Oregon, 1998.
49. A. Yasmin, J. L. Abot, and I. M. Daniel, *Scripta Materialia*, **49**, 81 (2003).
50. W. D. Callister and D. G. Rethwisch, "Materials Science and Engineering", Vol. 5, pp.634-680, John Wiley & Sons, NY, 2011.